Macromolecules

ARTICLE

pubs.acs.org/Macromolecules

Viscoelastic and Mechanical Behavior of Hydrophobically Modified Hydrogels

Jinkun Hao and R. A. Weiss*

Department of Polymer Engineering, University of Akron, 250 South Forge Street, Akron, Ohio 44325-0301, United States

ABSTRACT: The viscoelastic and mechanical behaviors of physically cross-linked copolymer hydrogels synthesized from *N*,*N*-dimethylacrylamide (DMA) and 2-(*N*-ethylperfluorooctane sulfonamido)ethyl acrylate (FOSA) with varying FOSA concentration were studied by rheological and static tensile tests. The strong hydrophobic association of the FOSA moieties in an aqueous environment produced core−shell nanodomains that provided the physical cross-links. These PDMA−FOSA hydrogels exhibited excellent mechanical properties, including a modulus of ∼130−190 kPa, elongation at break of 1000−1600%, and ∼500 kPa tensile strength, depending on the FOSA concentration. The physical gels were more viscous than comparable chemical gels and were much more efficient at dissipating stress. The latter characteristic produced relatively high tensile toughness, ∼4−6 MPa, because of the extra energy dissipation mechanism provided by the reversible, hydrophobic cross-links. The PDMA−FOSA hydrogel exhibited peculiar dynamic behavior which was greatly dependent on temperature. At 25 °C, the hydrogel was highly elastic, but as the temperature increased, its viscous behavior increased and a crossover of the dynamic moduli (i.e., $G'' > G'$) occurred at 55 °C, as the rheological characteristics of the material went from a viscoelastic solid to a viscoelastic liquid. That behavior is a consequence of the physical nature of the structure of the physical cross-links and the dynamic nature of hydrophobic associations, which are influenced by composition, temperature, and time.

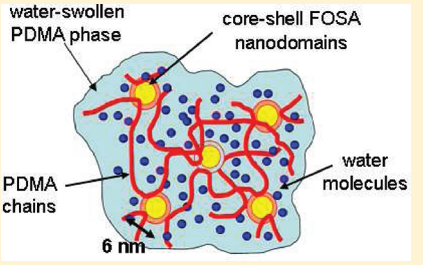

INTRODUCTION

Hydrogels are elastic polymer networks that absorb large amounts of water. Their porous microstructure and three-dimensional network structure provide good permeability and mechanical properties, respectively.[1] Typical hydrogels are prepared by chemical[2−4] or physical cross-linking[5−10] of hydrophilic polymers, such as polyacrylamide, poly(ethylene oxide), or poly(2-hydroxyethyl methyl acrylate). Chemical cross-linked hydrogels are formed from covalent bonds, and thus, they have a permanent shape that can be deformed by the application of stress, but which can also be recovered when the stress is removed if the stress is low enough. Because of the irreversible feature of a covalent bond,[11,12] such hydrogels cannot be manufactured into controlled shapes by melt processing methods such as injection molding or compression molding, except for cases where the covalent network is formed during that process.

Physical gels have transient cross-links formed by interchain associations involving complementary functional groups that exhibit, for example, electrostatic interactions, hydrophobic interactions, and hydrogen bonding or produce crystallizing segments.[6,8,13−17] Although those materials do not possess a permanent network structure, they do exhibit elasticity if the relaxation time of the network is much longer than the application time of stress. That is, physical elastic networks can be achieved when the stresses are either small, the temperature is sufficiently low, or the stress application is of short duration (i.e., short time or high frequency). Under such conditions, a physical gel may be mechanically indistinguishable from a covalent gel, and the network appears to be permanent. However, because of the reversible nature of noncovalent intermolecular interactions, physical hydrogels can be melt processed into a desired shape.[9] The reversible aspect of the network structure provides unique properties, such as viscous flow above a critical stress or time that allows the gel to be injectable and improved mechanical toughness compared with a covalent gel. Because of these special properties, physically cross-linked hydrogels have applications in such diverse technologies as injection moldable contact lenses, injectable drug delivery systems, scaffolds for tissue engineering, and oil field chemicals such as drilling muds.[17−19]

In general, gels that are highly swollen by a liquid are very weak because they do not have many intrinsic mechanisms to dissipate energy during their deformation. To obtain a hydrogel with a high degree of mechanical toughness, one needs to introduce additional dissipative mechanisms at the molecular level.[13,20,21] Gong and co-workers[22] demonstrated dramatic improvements of the strength of hydrogels by forming a "double network" of covalent cross-links. More recently, Abdurrahmanogluit et al.[5] reported that hydrophobic modification of a covalently cross-linked polyacrylamide hydrogel produced a large increase in extensibility and toughness as a consequence of the additional energy dissipation due to deformation of the hydrophobic associations, i.e., temporary junctions in the hydrogel due to aggregation of the hydrophobic species.

Received: September 20, 2011
Revised: November 5, 2011
Published: November 18, 2011

The work described in this paper is an extension of our prior work on physical cross-linking of poly(alkylacrylamide) hydrogels using strong hydrophobic interactions.[23−25] These materials are single physical-network hydrogels, as opposed to the double network (covalent + physical cross-links) hydrogel described by Abdurrahmanogluit et al.[5] In addition, a major difference between our system and that described in ref 5 is the use of a fluoroacrylate as the hydrophobic modifier in our hydrogels. The hydrophobic associations of fluorocarbon hydrophobes in a water medium are much stronger than for a hydrogenated hydrophobe,[26−29] and fluorocarbon groups possess excellent chemical and biological inertness, good thermal stability, high gas solubility (relative to water), high fluidity, and low surface energy, which are useful for biomedical applications.[30,31]

The materials described in this paper were physically cross-linked copolymer hydrogels synthesized from *N*,*N*-dimethylacrylamide (DMA) and 2-(*N*-ethylperfluorooctane sulfonamido)ethyl acrylate (FOSA) (see Scheme 1). Above a FOSA concentration of 5 mol %, the copolymers were insoluble in water because of the physical cross-links that arise from intermolecular associations of the hydrophobic species. The DMA portion of the copolymer is hydrophilic, so that these copolymers form highly swollen hydrogels when immersed in water.[23,24] Tian et al.[25] characterized the microstructure of the copolymer (PDMA−FOSA) hydrogels using small-angle neutron scattering (SANS), and a schematic model of the microstructure is shown in Figure 1.

Aggregation of the FOSA moieties produces a physically cross-linked microstructure of core−shell nanodomains, which are composed of a FOSA core surrounded by a water-depleted shell of DMA. The water-poor shell of the DMA is presumably comprised of the chain segments attached to the FOSA repeat units that have restricted mobility due to the covalent attachment to the FOSA aggregates. These core−shell nanodomains constitute the cross-link junctions in the physical hydrogel that is essentially water-swollen PDMA. The core−shell nanodomain size (core radius + shell thickness) is ∼6 nm.

The objective of the current study was to investigate the viscoelastic and mechanical properties of the PDMA−FOSA hydrogels. Rheological and tensile test results indicate that this physical hydrogel exhibits high mechanical strength, high extensibility, and reversible deformation. The viscoelastic behavior was characterized by stress relaxation experiments, and the temperature sensitivity of the physical cross-link structure was studied using dynamic oscillatory shear test. It is important to note that while physical cross-links provide gel-like properties (i.e., typical of a cross-linked polymer), the polymers can also exhibit properties typical of linear polymers when the reversible nature of the cross-links is exploited. That is a key aspect to the results and discussion that follow in this paper. However, the term "gel" is loosely applied in this paper to identify the copolymers. It is noted by the discussion of the mechanical properties when the copolymers are elastic solids (i.e., cross-linked gels) and when they exhibit viscous flow typical of liquids.

EXPERIMENTAL DETAILS

Materials. The PDMA−FOSA copolymers were previously synthesized by Dr. Jun Tian.[24] *N*,*N*-Dimethylacrylamide (DMA, 99%) and 2-(*N*-ethylperfluorooctane sulfonamido)ethyl acrylate (FOSA) were purchased from Sigma-Aldrich Chemical Co. and 3M Co., respectively. PDMA−FOSA was synthesized by free-radical polymerization of DMA and FOSA in dioxane. The characteristics of these copolymers are listed in Table 1. The sample nomenclature used is DF*x*, where DF indicates a copolymer of DMA and FOSA and *x* denotes the mol % of FOSA rounded to an integer value.

Scheme 1. Synthesis of PDMA−FOSA Copolymers

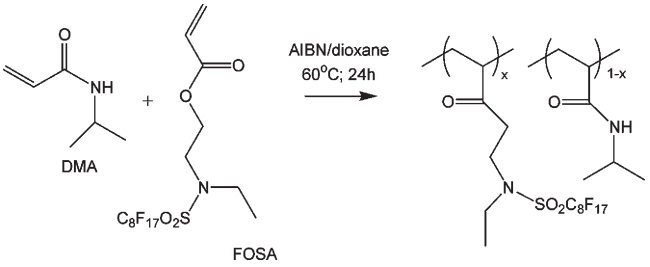

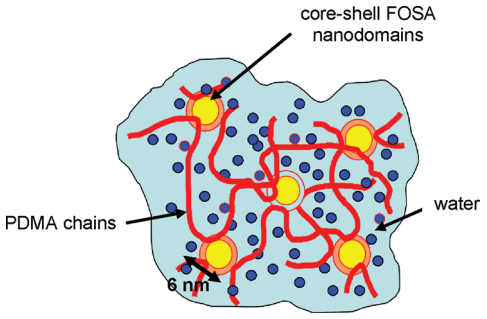

Figure 1. Schematic of core−shell structure of a water-swollen PDMA−FOSA hydrogel.

Table 1. Characteristics of the PDMA−FOSA Copolymers

polymer ID	FOSA (mol %)	DMA (mol %)	MBBA (mol %)	T_g (°C)	M_w (10^4 Da)	M_n (10^4 Da)
DF5	4.9	95.1	0	106	7.3	3.8
DF9	9.0	91.0	0	96	5.6	2.9
DF22	22	78.5	0	81	7.6	5.1
PDMA	0	96.0	4.0	144		

The hydrogel samples were prepared by compression-molding dry PDMA−FOSA copolymer films at 150−180 °C under vacuum and then immersing the films in deionized water for 7 days to ensure equilibrium hydration. A covalently cross-linked PDMA was synthesized for comparison to the physical hydrogels. *N*,*N*′-Methylenebis(acrylamide) (MBAA) was obtained from Sigma-Aldrich, purified by recrystallization twice in methanol, and incorporated into a PDMA to provide cross-linking sites. A photoinitiator, Irgacure 2959 (2-hydroxy-4′-(2-hydroxyethoxy)-2-methylpropiophenone), was obtained from Sigma-Aldrich and used as received. DMA, MBAA, and Irgacure 2959 were codissolved in deionized water using a monomer concentration (DMA + MBAA) of 20 wt % and the photoinitiator concentration of 0.4 wt %; the content of MBAA in monomers was 4 mol %. The solution was then transferred to a reaction dish, degassed, and radiated with a UV lamp with a 365 nm wavelength for 5 min. Covalently cross-linked hydrogels were obtained from the resultant polymer by immersing in deionized water for 3 days.

Rheological Measurements. Oscillatory shear, steady shear, and stress relaxation measurements were made with a TA Instruments ARES-G2 rheometer equipped with 8 mm parallel plates. A fixture with a water trap was used to keep the sample hydrated. The linear response region for the dynamic experiments was determined with a strain sweep.

Table 2. Swelling Ratios and Cross-Link Densities of Physical and Chemical Gels at Room Temperature (~25 °C)

sample ID	DF5-eq	DF9-eq	DF22-eq	DF5-70	DF9-67	PDMA chemical gel
FOSA conc (mol %)	4.9	9.0	22	4.9	9.0	0
swelling ratio (water/polymer)	290	170	69	70	67	490
v_2 (vol fraction polymer)	0.23	0.33	0.54	0.55	0.55	0.15
ν_e (mol m^{-3}) at 100 rad s^{-1}	190	370	650	410	930	99
ν_e (mol m^{-3}) at 1 rad s^{-1}	130	280	300	230	640	95

Dynamic experiments were performed within a frequency range of 0.1−100 rad s^{-1} using a strain amplitude of 0.5%. Steady shear experiments were performed within a shear rate range of 0.001−100 s^{-1}. For the shear stress-relaxation experiments, a step shear strain was first applied to the sample, and the isothermal stress relaxation was then followed for a 20 min period.

Tensile Tests. Tensile tests were carried out with an Instron universal testing machine, Model 5567, using a 100 N load cell. The samples were cut into a dumbbell shape, with a gauge length of 7.620 mm and width of 3.175 mm. The engineering tensile strain was used, defined as the change in the length divided by the undeformed length of the specimen. The engineering stress was obtained by dividing the force by the original cross-sectional area of the specimen.

RESULTS AND DISCUSSION

The PDMA−FOSA copolymer films absorbed large amounts of water to form hydrogels. As the concentration of the hydrophobic FOSA in the copolymer increased, the effective cross-link density of the gel increased and the equilibrium amount of water absorbed decreased (see the first three data columns in Table 2). The equilibrium swelling ratio ranged from 69 to 290 (defined as mass of water/mass of polymer) as the FOSA concentration increased from 4.9 to 22 mol %. The hydrogel samples that were fully equilibrated with water are hereafter denoted as DF*x*-eq, where *x* is the integer value of the FOSA concentration in mol %. Also listed in Table 2 are two hydrogels that were only partially swollen to achieve approximately the same water concentration as the equilibrium value for DF22-eq. Those two samples are denoted as DF*x*-*y*, where *y* is the water concentration denoted by the swelling ratio. Thus, these two samples and DF22-eq represent a series of hydrogels with similar water concentrations but varying FOSA concentration.

Dynamic Viscoelastic Behavior. The frequency dependence of the dynamic storage (G') and loss (G'') shear moduli of the PDMA−FOSA hydrogels at room temperature and equilibrium and partial hydration are shown in Figure 2. For all the hydrogels, G' was greater than G'' over the entire frequency range, which is consistent with the solidlike, elastic nature of the gel. The weak dependence of G' and G'' with frequency is due to the physical, nonpermanent nature of the network.[8,19] The network underwent some creep, which provided a viscous, energy dissipative response, but for most part, the gels were still elastic at room temperature due to the long relaxation time of the physical hydrophobic interactions.

The upturn in G'' at the lower frequencies suggests the onset of a structural change in the gel network, which is most likely viscous flow. That is expected for a physical gel when the experimental time frame during which the stress is applied becomes comparable to the relaxation time of the gel—in this case, at the lower test frequencies. The frequency dependence of the shear modulus of the PDMA chemical gel is also shown in Figure 2. G' and G'' were much lower than those for the PDMA−FOSA physical gels, and for the PDMA chemical gel, the moduli were nearly independent of frequency as would be expected for a covalent network.

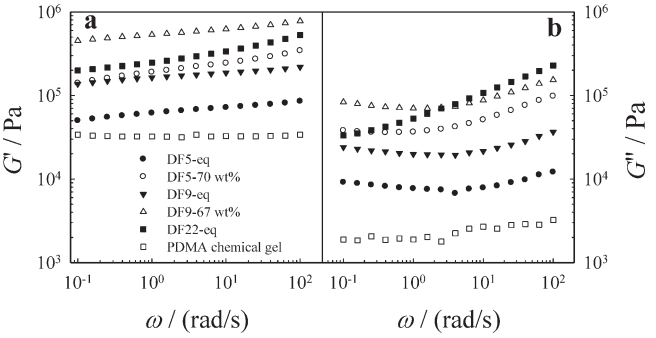

Figure 2. (a) Storage modulus, G', and (b) loss modulus, G'', at 25 °C as a function of frequency for PDMA−FOSA hydrogels with different FOSA and water concentrations and PDMA chemical gel (strain = 0.5%).

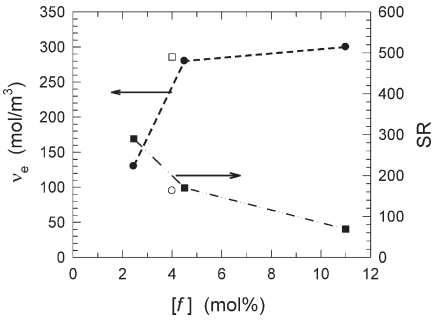

Figure 3. Cross-link density and water swelling ratio for (●, ■) PDMA−FOSA hydrogels and (○, □) chemically cross-linked PDMA hydrogel.

The dynamic storage modulus, G', for the PDMA−FOSA hydrogels was in the range of 50−500 kPa, which is a relatively high modulus for a hydrogel. For example, the reported G' for chemically cross-linked poly(acrylamide) hydrogels is 100 Pa−5 kPa for a cross-linker concentration in the range of 0.3−5.0 mol %[11] and 100 Pa−10 kPa for polyacrylamide−clay nanocomposite hydrogels when the clay contents are in the range of 0.2−7% (w/v).[32] Similarly, G' for the PDMA chemical gel was only ~30 kPa, even though its functionality was much greater than that of DF5 (see Figure 3).

Hydrophobically modified hydrogels prepared by Abdurrahmanogluit et al.[5] with a concentration of the hydrophobic species of 5 mol % had a storage modulus of 1−3 kPa. Those materials were synthesized using a hydrogenated hydrophobe, in contrast to the fluorinated monomer used in this study. The significantly higher G' values observed for the PDMA−FOSA hydrogels are a consequence of the stronger hydrophobic associations of fluorinated groups in a water environment compared with hydrogenated groups.[27,28,33] For PDMA−FOSA, the strong interactions of the fluorinated hydrophobes produced a higher effective cross-link density due to the aggregation of the fluorinated hydrophobes into nanometer-size domains.[24,25]

G' increased with increasing FOSA content, which is partly due to the effect of the increase in cross-link density but also due to the decrease in equilibrium swelling of the gel. However, even when the water swelling ratio was nearly 300% (sample DF5-eq), the modulus was still greater than 50 kPa. For a phantom network, the elastic shear modulus, G, of a gel is related to the cross-link density ν_e and the extent of solvent swelling by eq 1[34]

$$G = \left(1 - \frac{2}{\phi}\right)\nu_e RT{\nu_2}^{2/3} \quad (1)$$

where ν_2 is the volume fraction of cross-linked polymer in the hydrogel, R and T are the gas constant and absolute temperature, respectively, and ϕ is the functionality of the cross-links that is assumed here to be 4. ν_2 was calculated from eq 2[35]

$$\nu_2 = \left[1 + \frac{(q_F - 1)\rho}{d}\right]^{-1} \quad (2)$$

where q_F is the mass of swollen gel divided by mass of dried gel, ρ is the polymer density (DF5: 1.19 g mL^{-1}; DF9: 1.23 g mL^{-1}; and DF22: 1.26 g mL^{-1}), and d is the solvent density (1.00 g mL^{-1}). The cross-link densities calculated from eqs 1 and 2 are listed in Table 2. Since the shear moduli varied with frequency, calculations of the cross-link density were made from G' at high frequency (100 rad s^{-1}) and low frequency (1 rad s^{-1}) (see Table 2).

The effects of FOSA and water concentrations on the modulus were separated by comparing the viscoelastic response of samples with varying FOSA content, but the same amount of water; cf. the data for samples DF22-eq, DF9-67, and DF5-70 in Figure 2, which have swelling ratios of ∼70%. For equivalent amounts of water, $G'_{DF9\text{-}67} > G'_{DF22\text{-}eq} > G'_{DF5\text{-}70}$. That reflects the contribution of the increased cross-link density of the gel, which appears to account for about half of the total increase in the modulus of the gel with increasing FOSA content—the decrease in equilibrium water content accounting for the other half of the increase in G'. As FOSA increased from 5 to 9 mol %, the cross-link density increased because the contribution of more FOSA groups. When the FOSA concentration increased further, however, to 22 mol % for the same amount of water as the samples with the lower FOSA concentration, the cross-link density decreased (see Table 2). That result was unexpected, since one would expect that the cross-link density should increase with fixed water concentration and increasing FOSA concentration. The reason for this is not known, but perhaps it is related to blockiness that may occur in the FOSA distribution for the higher FOSA concentratons. That explanation, however, is simply speculation, and further investigation of this phenomenon is needed.

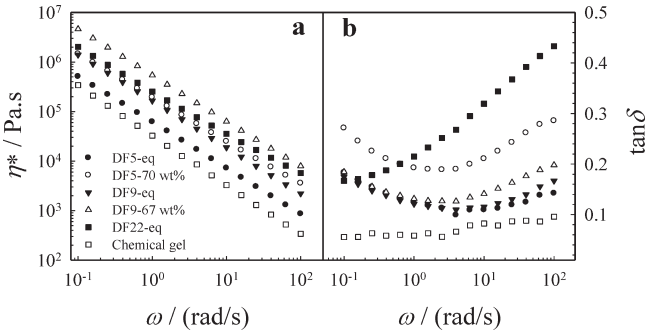

Figure 4. (a) Complex viscosity η^* and (b) loss factor tan δ as a function of frequency at 25 °C calculated from the data in Figure 2 for PDMA−FOSA hydrogels with different FOSA and water concentrations (strain = 0.5%).

It is not obvious how best to compare the properties of physical gels with a covalent gel. One might consider comparing samples with equivalent cross-link density, functionality, or water content. Although those three quantities are simply related for a covalent gel, that is not the case for the physical gel. The microphase separation that occurred in the PDMA−FOSA hydrogels produced higher than expected cross-link density due to the multiple network chains that were associated with a single nanodomain. We chose to make the comparison of the different hydrogels on the basis of a "theoretical" cross-link concentration, $[f]$. That is, one MBAA molecule produces a single cross-link site in the covalent gel, while two FOSA molecules are needed to produce a bimolecular hydrophobic interaction that results in a simple, physical cross-link. In that case, $[f]$ for a FOSA composition of 8 mol % would be equivalent to $[f]$ for an MBAA composition of 4 mol % in the covalently cross-linked PDMA, all else being equal. We recognize the limitations in this strategy, but similar problems in comparing the two types of gels occur with whatever parameter is chosen as the independent variable.

Figure 3 plots the cross-link density, ν_e, calculated from the $G'(\omega)$ at room temperature (frequency, ω = 1 rad/s) and the swelling ratio for the physical and chemical hydrogels as a function of the theoretical cross-link concentration. As might be expected, for the physical gel, ν_e increased with increasing FOSA concentration (note that this result differs from the data for fixed water concentration discussed earlier in the paper). The datum point for the covalent PDMA gel in Figure 3 is close to that of DF9-eq, yet ν_e for the PDMA gel was nearly 3 times lower and SR was 3 times higher than for DF9-eq. That result also demonstrates the difference between these physical gels and conventional covalent gels as well as underscoring the difficulty in formulating meaningful comparisons.

Figure 4 shows the frequency dependence of the complex viscosity and loss factor (tan $\delta = G''/G'$) for the PDMA−FOSA hydrogels and PDMA chemical gel. For the chemical gel, log η^* was a linear function of log ω, and the slope was −1.0. That is indicative of an infinite relaxation time or that the relaxation time of the network is very long compared with the experimental time frame, which is expected for a permanent network. For the PDMA−FOSA physical gels, the |slope| < 1.0 (see Table 3), which is a consequence of some relaxation of the network.

As shown in Figure 4b, tan δ for the physical hydrogels ranged from ∼0.1 to 0.4, which also indicates a finite viscous contribution to the mechanical behavior of those hydrogels. In contrast, tan δ of the covalently cross-linked PDMA gel ranged was much

less frequency sensitive, though it did vary from ~0.05 to 0.1 over the range of frequencies studied. For a perfect covalent gel, tan δ should be zero, so the finite values measured in this study indicate that these gels probably have imperfections (e.g., dangling chains, un-cross-linked chains, and/or loops that do not support stress) that produce some viscous response to the deformation. The key difference, however, between the two types of gels is that the more significant viscous character of the physical gels should provide improved energy damping ability of these gels over a wide frequency range.

The nonlinear dynamic response of the DF9-eq hydrogel is shown in Figure 5. In this case, the frequency was held constant at 1 rad/s and the strain amplitude was varied from 0.3 to 120%. Upon completing the strain sweep, the strain amplitude was reduced to 0.5%, the time dependence of the complex moduli was followed for about 4 min, and then the strain sweep was repeated. Figure 5 shows three strain sweep−time sweep cycles. Figure 5a1 shows the time-dependent response of the material prior to the first strain sweep. G' and G'' were independent of time, indicating no change in the structure of the hydrogel for a strain of 0.5%. For these test conditions, the DF9-eq hydrogel behaved as a viscoelastic solid (i.e., $G' > G''$) with tan $\delta \sim 0.1$.

The first strain sweep, Figure 5b1 shows that the linear response of the gels persisted to a strain of about 2%. Above ~2% strain, G' decreased by 2 orders of magnitude, and G'' first increased, then exhibited a maximum, and decreased. The value of G'' also became larger than that of G' at a strain of ~47%, and that crossover signifies a solid (gel) to liquid transition. That is, the structure physical cross-links that provided the solidlike behavior of the hydrogel were sufficiently disrupted by the large strains so that the material exhibited viscous flow. However, when the strain was reduced to 0.5%, the structure and the elastic behavior was almost instantaneously recovered (Figure 5a2); i.e., a liquid to gel transition occurred as soon as the nonlinear strain was removed. This reversibility of the structure and the gel to liquid transition behavior was reproducible through at least three successive stain sweep cycles (Figure 5 (b1/a2; b2/a3; b3/a4)). The only distinctive difference in the behavior during the three cycles was that for the second and third cycles the strain (14%, 12%) at which the gel to liquid transition was about 25−30% of that observed in the first cycle. That lack of reproducibility in the position of the gel−liquid transition may simply be due to experimental errors in the stress measurement, but it may also signify some conditioning of the gel occurred in the first deformation cycle. Additional work is necessary to determine if those difference are significant.

Table 3. Slope of log η^* vs log ω for the Hydrogel Samples in Figure 4a

sample	DF5-eq	DF9-eq	DF22-eq	DF9-67	DF5-70	chemical gel
slope	−0.93	−0.94	−0.85	−0.93	−0.88	−1.0

Steady Shear Behavior. Figure 6 shows the shear rate dependence of the viscosity, η, for fully hydrated PDMA−FOSA hydrogels at 25 °C. At low shear rates, the slope of the viscosity data in Figure 6 for each sample is about −1. That value indicates that the viscosity goes to infinity at zero shear rate, which is consistent with the properties of an elastic solid;[36] i.e., viscous flow did not occur over that region of share rate. At higher shear rates, however, the viscosity curve becomes nonlinear, which indicates viscous flow. For each material, the viscosity decreased by 5−6 orders of magnitude as the hydrophobic species pulling out of the nanodomains, which allows chain translation to occur. Similar observations for physical gels have been reported by Angelopoulos et al.[6] and by Sui et al.[8] This flow behavior under nonlinear deformation conditions contrasts with the linear viscoelastic behavior, which was primarily elastic (see Figure 2).

As the FOSA content increased (and water content decreased), the η increased by an order of magnitude and the gels became stiffer. In general, these hydrophobically associated hydrogels

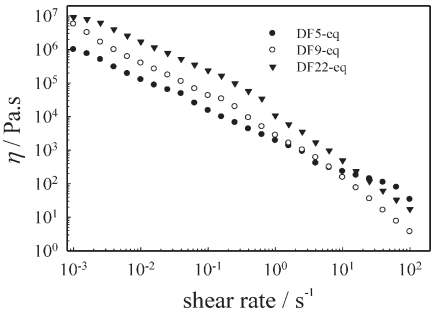

Figure 6. Steady-state shear viscosity, η, at 25 °C as a function of shear rate for the PDMA−FOSA hydrogels fully equilibrated with water.

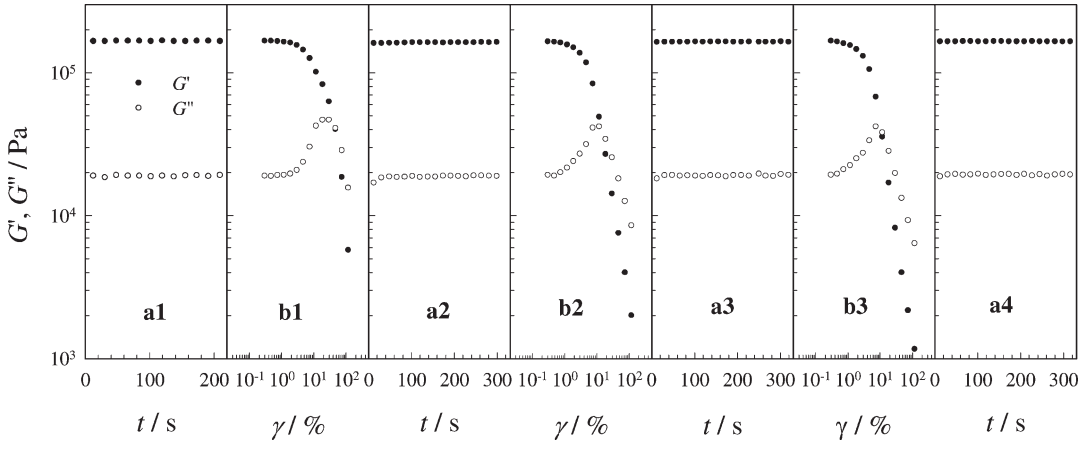

Figure 5. Strain sweep cycles at 25 °C for DF9-eq for (a1, a2, a3, a4) time dependence of G' and G'' with strain = 0.5% and ω = 1 rad/s; (b1, b2, b3) strain dependence of G' and G'' with ω = 1 rad/s.

dx.doi.org/10.1021/ma202130u |Macromolecules 2011, 44, 9390–9398

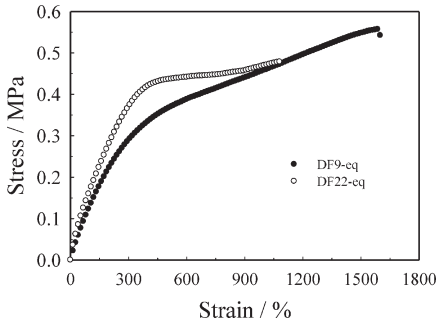

Figure 7. Tensile stress−strain curves of fully hydrated PDMA−FOSA hydrogels at 23 °C.

Table 4. Mechanical Properties of PDMA−FOSA Hydrogels with Equilibrium Water Concentration[a]

sample	modulus (kPa)	utlimate stress (kPa)	extension at break (%)	toughness (kPa)
DF9-eq	130	560	1600	6300
DF22-eq	190	480	1100	4100

[a] The extension rate was 30.48 mm min^{-1}.

were thixotropic and the network structure was reversible. The network was disrupted by nonlinear stresses, but the structure quickly recovered after the stress was removed.

Mechanical Properties. Tensile stress vs strain curves for the DF9-eq and DF22-eq hydrogels are shown in Figure 7, and the properties are summarized in Table 4. The PDMA chemical gel and DF5-eq hydrogel films were too weak for tensile measurements. The DF9 and DF22 hydrogels exhibited high modulus (∼130−190 kPa), high elongation to break (1100−1600%), and high ultimate tensile strength (480−560 kPa). The high modulus is a consequence of the high cross-link density (Table 2), which is due to the multifunctional cross-link character of the hydrophobic nanodomains, and the high strength and elongation is attributed to ability of the physical cross-links to dissipate energy. When a crack occurs, the reversible disengagement of the hydrophobic associations can dissipate the crack energy and suppress the macroscopic growth of the crack,[5] which, in turn, produces high toughness of the hydrogel. Note that the ultimate stress and elongation at break of these PDMA−FOSA hydrogels were much greater than the properties that Abdurrahmanogluit et al.[5] reported for their double network hydrogels that used a hydrogenated hydrophobe and covalent cross-links (∼70 kPa ultimate stress and ∼300% ultimate elongation). The difference is a consequence of the much stronger hydrophobic association induced by fluorocarbon hydrophobes compared with hydrocarbon analogues. For the latter materials, no microphase separation was reported.

Although tensile tests were not performed with the DF5-eq hydrogel, it was clear from handling the material that the DF9-eq gel was much tougher. However, the toughness (the area under the stress−strain curve) of the DF22-eq gel was lower than that of the DF9-eq material. Both samples exhibited yield points, though the stress at yield was larger for the DF22-eq sample (see Figure 7) due to the higher cross-link density (Table 2). The lower toughness for the D22-eq was mainly due to a lower elongation at break that may

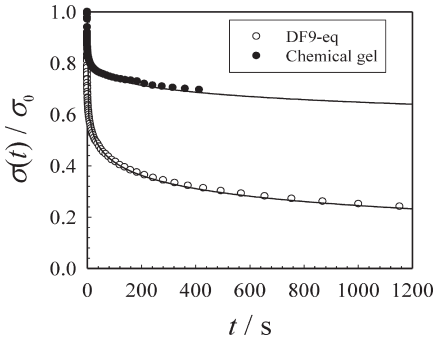

Figure 8. Stress relaxation response for DF9-eq and a PDMA chemical gel following a step strain of 1.0%. The solid line is the least-squares fit of eq 3.

be a consequence of the higher cross-link density and lower water content, which made the sample more brittle.

Stress Relaxation. The dissipation of energy for a fixed deformation is manifest by stress relaxation.[16,37,38] Figure 8 shows the stress relaxation response at 23 °C for the DF9-eq hydrogel and the PDMA covalently cross-linked hydrogel (cross-linker: MBAA, 0.5 mol%) following a step strain of 1%. Each material showed a two-stage stress relaxation response: a fast decrease in stress for short times after the step strain, followed by a slow relaxation covering a couple of decades of time. The total stress relaxation was significantly higher for the physical gel. For the chemical gel, the stress relaxation is due primarily to changes in the conformation of the network chains, while for the physical gel, in addition to relaxation of the network chains, there is a relaxation associated with changes in the gel structure as chains disengage from the nanodomains. The dynamics associated with the later mechanism is related to the average lifetime of a cross-link junction. If a network is perfect and irreversibly cross-linked, no relaxation should occur and the relaxation time should be infinite.[39]

The data in Figure 8 cannot be represented by a single relaxation time. A distribution of relaxation times usually occurs in polymers and polymer networks due to the distribution of network chain lengths and the topology of the network junctions. For a microphase-separated polymer, there are additional relaxation processes that are associated with the nanodomains. The data in Figure 8 are not sufficient for determining the entire relaxation time spectrum for the gels. Instead, a stretched exponential[40] was fit to the data

$$\frac{\sigma}{\sigma_0} = e^{-(t/\lambda)^{\beta}} \tag{3}$$

where λ is a mean relaxation time and β is related to the moments, n, of the relaxation time distribution as in eq 4

$$\langle \tau^n \rangle = \int_0^{\infty} t^{n-1} e^{-(t/\lambda)^{\beta}}\, dt \tag{4}$$

This approach has been used successfully by Gurlovenko and Gotlib[41] and by Baeurle et al.[42] to model the stress relaxation behavior of cross-linked networks with transient cross-links.

The fits of eq 3 to the data in Figure 8 are shown by the solid curves, and the fitting parameters are summarized in Table 5. The mean relaxation time for the chemical gel was 3 orders of magnitude greater than for the physical gel, and correspondingly, the stress in the chemical gel is dissipated much more slowly. As stated earlier, a perfect chemical gel should have an infinite relaxation time, so the finite relaxation time of the PDMA chemical gel supports the earlier conclusion based on the finite value of tan

Table 5. Fitting Parameters Calculated from eq 3 for the Data in Figure 7

sample	λ (s)	β	r^2
PDMA	2.10×10^5	0.156	0.95
DF9-eq	1.86×10^2	0.203	0.97

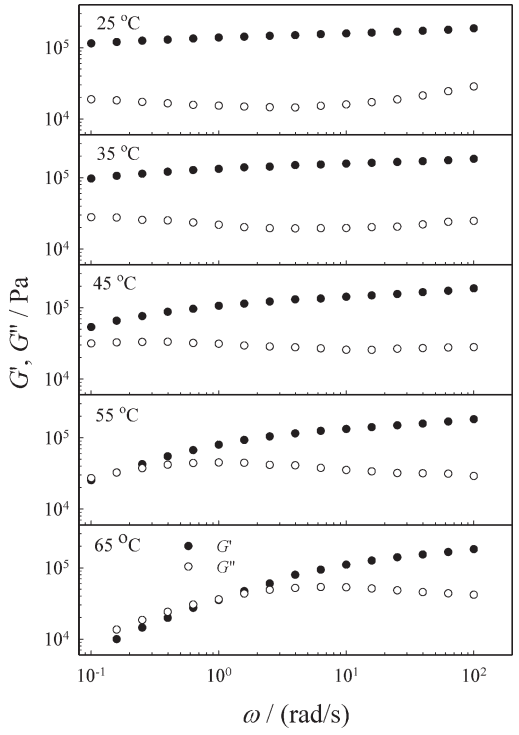

Figure 9. Frequency dependence of the storage moduli, G', and loss moduli, G'', for DF9-eq at temperatures between 25 and 65 °C.

δ that this network contains imperfections that do not support stress.

For the chemical hydrogel, the stress decays very slowly at longer times, which is not effective for dissipating energy quickly. In contrast, the stress decreases more rapidly in the DF9-eq gel, and even after 20 min, the stress continued to decay. The quicker stress relaxation provides a mechanism for dissipating energy quickly, which is consistent with the higher toughness measured for the physical hydrogels.

Temperature Influence on the Behavior of PDMA−FOSA Hydrogels. Figure 9 shows the temperature dependence of G' and G'' for the DF9-eq hydrogel. At 25 °C, G' decreased as the frequency decreased. As the temperature increased, the slope of log G' vs log ω increased; i.e., at higher temperature G' decreased faster with decreasing frequency. The difference between G' and G'' at low frequency became smaller as temperature increased from 25 to 55 °C, and at 55 °C, a crossover between G' and G'' occurred at a frequency of ~0.16 rad s^{-1}. The crossover frequency increased with increasing temperature.

The network structure of the PDMA−FOSA hydrogels is a consequence of strong hydrophobic associations that produce microphase separation of FOSA nanodomains. The driving forces for gelation are the attractive interactions between the hydrophobic groups and the repulsive interactions between the FOSA groups and water. The activation energy for the disengagement of

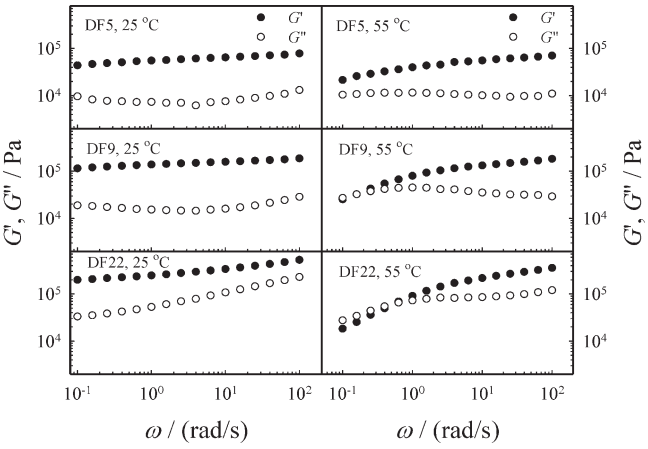

Figure 10. Frequency dependence of G' and G'' of the PDMA−FOSA hydrogels at 25 and 55 °C.

hydrophobic associations is of the order of the thermal energy kT, so that the free and associated hydrophobes in such hydrogels are in a dynamic equilibrium.[5]

Since the T_g of poly(FOSA) is 45 °C, the FOSA nanodomains in a PDMA−FOSA hydrogel are glassy at room temperature, and the relaxation time for dissociation of FOSA−FOSA interactions is expected to be relatively long, even when the hydrogel is stressed. As a consequence, below the T_g of the FOSA nanodomains (i.e., the data corresponding to 25 and 35 °C in Figure 9), the hydrogel behaves elastically (i.e., solidlike) and the network structure, as measured by G', is relatively insensitive to the frequency of the deformation, ω. $G' \gg G''$ as long as the stress amplitude is sufficiently low and/or the gel relaxation time is much greater than the experimental time, $t \sim 1/\omega$. As temperature increases to $>T_g$ of the FOSA nanophase, the flexibility of the hydrophobic domains increases and the relaxation times of the domains decrease. As a result, the network structure, which is held together by the hydrophobic FOSA nanodomains, becomes more sensitive to the time for which stress is applied. G' decreases with decreasing frequency, since lower frequency corresponds to longer experimental times.

The decrease in the elastic behavior of the gel (i.e., G') is accompanied by an increase in the viscous character, G''. At sufficiently high temperature and sufficiently low frequency, G' and G'' become similar and eventually the two quantities cross over and G'', the viscous response of the gel, becomes dominant. The crossover corresponds to a transition from solidlike to liquidlike behavior of the gel,[43] which in this case is due to a disruption of the physical network composed of hydrophobic associations.

Unlike a chemical gel, the gelation phenomenon for a physical gel is reversible. As such, it can be used to develop self-healing properties or, if a second network were introduced, e.g., a chemical network, shape memory hydrogels should be possible. For the latter application, a temperature or stress application could be used to disengage the hydrophobic associations, i.e., the temporary network, and a temporary shape could be fixed by either cooling the deformed sample while under load or by lowering the stress so that the physical network re-forms. Shape recovery should occur when the gel in its temporary shape is reheated and/or by the application of a sufficiently large stress that can break the physical network. From a molecular perspective, the shape memory cycle involves controlling the relaxation

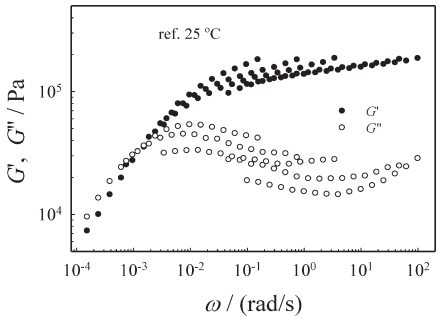

Figure 11. Failure of time−temperature superposition of the viscoelastic properties of the DF9-eq hydrogel. The reference temperature is 25 °C.

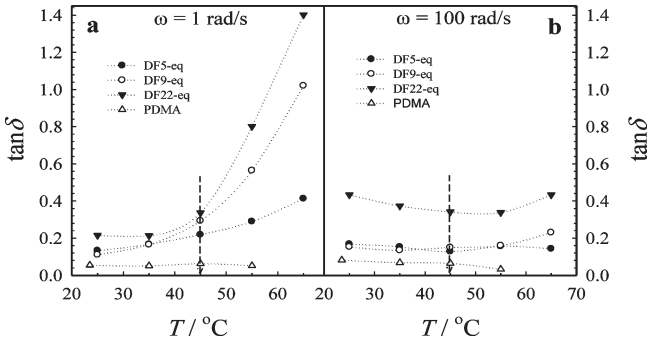

Figure 12. Tan δ vs temperature for PDMA−FOSA and PDMA hydrogels at frequencies of (a) 1 rad s^{-1} and (b)100 rad s^{-1}. The dashed arrow denotes the T_g of poly(FOSA).

times of the temporary network using stress amplitude and/or temperature.

Figure 10 compares G' and G'' of the three fully swollen PDMA−FOSA hydrogels at temperatures below (25 °C) and above (55 °C) the T_g of the FOSA nanodomains. At 25 °C, the difference between G' and G'' first increases, but then decreases as the frequency was reduced. At 55 °C, above the T_g of poly(FOSA), the difference between G' and G'' becomes distinctively smaller than at 25 °C for all three hydrogels. For DF5-eq, there is no crossover of G' and G'' in the test frequency window, but when the FOSA content increases to 9 mol %, a crossover appears at $\omega \sim 0.16$ rad s^{-1}. When the FOSA concentration increases to 22 mol %, the crossover point moves to higher frequency, $\omega \sim 0.52$ rad s^{-1}.

Figure 11 shows the attempt to construct a viscoelastic mastercurve for DF9-eq using time−temperature superposition (TTS). The reference temperature was 25 °C. It is clear from these data that TTS failed, and the hydrogels were thermorheologically complex. Similar results were observed for the other two physical gels, and the source of the complexity of these materials was the microphase separation due to the hydrophobic associations in these systems.

Figure 12 shows the temperature dependence of the loss factor, tan δ, for the PDMA−FOSA hydrogel and the PDMA chemical gel (cross-linker: MBAA, 0.5 mol%) at frequencies of 1 and 100 rad s^{-1}. At the higher frequency, tan δ was relatively insensitive to temperature changes between 25 and 65 °C for both gels. The magnitude of tan δ, however, was significantly lower for the covalent gel than for the physical gels. For the physical gels, tan δ increased with increasing FOSA concentration, which corresponds to an increase in the viscous response, presumably as a consequence of increased volume fraction of the FOSA microphase. However, as was previously shown in Figures 9 and 10, the PDMA−FOSA hydrogels were viscoelastic solids at a high frequency of 100 rad s^{-1} for the entire range of temperatures studied.

At the lower frequency, 1 rad s^{-1}, tan δ of the covalent gel was independent of temperature, which is consistent with the elastic solid nature of that gel. For the physical gel, below the T_g of polyFOSA (45 °C), tan δ was small and relatively insensitive to temperature, which is consistent with a viscoelastic solid. Above 45 °C, however, tan δ increased rapidly with temperature, corresponding to viscous flow of the sample.

It was somewhat surprising that viscous flow was observed for the physical gels with the higher FOSA concentrations, since those two gels had the lowest water concentrations and the highest "theoretical" cross-link concentration. However, the hydrophobic interaction induced microphase separation of the FOSA is favored by high water concentration. As a result, the materials that showed the highest elastic properties (G', tensile modulus and tensile yield stress) below the T_g of polyFOSA also exhibited the greater liquidlike behavior above the polyFOSA T_g. The nonlinear properties (shear viscosity) of the hydrogels were also higher for the samples with the lower water concentrations.

CONCLUSIONS

High modulus, tough hydrogels were achieved with a copolymer of dimethylacrylamide, DMA (which forms a water-soluble polymer), and 2-(*N*-ethylperfluorooctane sulfonamido)ethyl acrylate (FOSA), a water-insoluble monomer. Incompatibility of the fluoroacrylate groups with the PDMA produces microphase separation of a hydrophobic nanophase that serves as a multifunctional physical cross-link. The addition of water further promotes microphase separation as a result of the repulsive interactions of the hydrophobe and water. The unusually high stiffness and toughness that are exhibited by the PDMA−FOSA hydrogels are due to a high cross-link density that results from the multifunctionality of the cross-links and the ability of these gels to dissipate energy when deformed because of a reversible disengagement of the hydrophobic groups from the nanodomains. That provides a viscous mechanism that produces stress relaxation and effective energy dissipation.

The strength of the physical hydrogels increases with increasing concentration of the hydrophobic species, though if the water concentration in the gel becomes too low, the hydrogel becomes more brittle.The physical nature of the gels also allows for viscous flow of the hydrogels if the stresses are sufficiently high or the time frame of the deformation sufficiently long (i.e., low frequency).

The temperature dependent dynamic behavior of the PDMA−FOSA hydrogels was unusual. At temperatures below the glass transition of the nanodomains (T_{gn}), G' was relatively insensitive to frequency, which is consistent with an elastic gel. However, when the temperature exceeded T_{gn}, G' and G'' were frequency dependent, and as frequency increased, a crossover occurred where G'' became larger than G'. The crossover represents a reversible gelation transition where, with decreasing frequency, the material changes from a viscoelastic solid to a viscoelastic liquid. At that point, the material exhibits viscous flow. That behavior is useful for designing an injectable hydrogel where a high stress or slow deformation can be used to achieve viscous flow, but gelation occurs when the stress is removed or sufficiently decreased. That phenomenon arises from the nanodomain structure

of the phydical cross-links for these materials and the dynamic equilibrium nature of the hydrophobic associations.

AUTHOR INFORMATION

Corresponding Author
*Tel 330-972-2581, Fax 330-972-5290, e-mail rweiss@uakron.edu.

ACKNOWLEDGMENT

This research was partially supported by a grant from the Polymer Program of the National Science Foundation (Grant DMR- 0960461).

REFERENCES

(1) Tanaka, Y.; Gong, J. P.; Osada, Y. *Prog. Polym. Sci.* **2005**, *30*, 1.
(2) Takigawa, T.; Yamawaki, T.; Takahashi, K.; Masuda, T. *Polym. Gels Networks* **1997**, *5*, 585.
(3) Sayil, C.; Okay, O. *Polym. Bull.* **2002**, *48*, 499.
(4) Xue, W.; Champ, S.; Huglin, M. B. *Polymer* **2001**, *42*, 3665.
(5) Abdurrahmanoglu, S.; Can, V.; Okay, O. *Polymer* **2009**, *50*, 5449.
(6) Angelopoulos, S. A.; Tsitsilianis, C. *Macromol. Chem. Phys.* **2006**, *207*, 2188.
(7) Patra, T.; Pal, A.; Dey, J. *Langmuir* **2010**, *26*, 7761.
(8) Sui, K. Y.; Gao, S.; Wu, W. W.; Xia, Y. Z. *J. Polym. Sci., Part A: Polym. Chem.* **2010**, *48*, 3145.
(9) Van Tomme, S. R.; Mens, A.; van Nostrurn, C. F.; Hennink, W. E. *Biomacromolecules* **2008**, *9*, 158.
(10) Cho, J. Y.; Heuzey, M. C.; Begin, A.; Carreau, P. J. *Biomacromolecules* **2005**, *6*, 3267.
(11) Abdurrahmanoglu, S.; Okay, O. *Macromolecules* **2008**, *41*, 7759.
(12) Sayil, C.; Okay, O. *Polymer* **2001**, *42*, 7639.
(13) Miquelard-Garnier, G.; Demoures, S.; Creton, C.; Hourdet, D. *Macromolecules* **2006**, *39*, 8128.
(14) Boucard, N.; Viton, C.; Domard, A. *Biomacromolecules* **2005**, *6*, 3227.
(15) Stahl, P. J.; Romano, N. H.; Wirtz, D.; Yu, S. M. *Biomacromolecules* **2010**, *11*, 2336.
(16) Pan, Y. S.; Xiong, D. S. *J. Mater. Sci.* **2010**, *45*, 5495.
(17) Nowak, A. P.; Breedveld, V.; Pakstis, L.; Ozbas, B.; Pine, D. J.; Pochan, D.; Deming, T. J. *Nature* **2002**, *417*, 424.
(18) Zhao, Y.; Yokoi, H.; Tanaka, M.; Kinoshita, T.; Tan, T. W. *Biomacromolecules* **2008**, *9*, 1511.
(19) Yan, H.; Frielinghaus, H.; Nykanen, A.; Ruokolainen, J.; Saiani, A.; Miller, A. F. *Soft Matter* **2008**, *4*, 1313.
(20) Haraguchi, K.; Takehisa, T. *Adv. Mater.* **2002**, *14*, 1120.
(21) Abdurrahmanoglu, S.; Okay, O. *J. Appl. Polym. Sci.* **2010**, *116*, 2328.
(22) Gong, J. P.; Katsuyama, Y.; Kurokawa, T.; Osada, Y. *Adv. Mater.* **2003**, *15*, 1155.
(23) Bae, S. S.; Chakrabarty, K.; Seery, T. A. P.; Weiss, R. A. *J. Macromol. Sci., Pure Appl. Chem.* **1999**, *A36*, 931.
(24) Tian, J.; Seery, T. A. P.; Weiss, R. A. *Macromolecules* **2004**, *37*, 9994.
(25) Tian, J.; Seery, T. A. P.; Ho, D. L.; Weiss, R. A. *Macromolecules* **2004**, *37*, 10001.
(26) Seery, T. A. P.; Yassini, M.; Hogenesch, T. E.; Amis, E. J. *Macromolecules* **1992**, *25*, 4784.
(27) Zhang, Y. X.; Da, A. H.; Hogenesch, T. E. *J. Polym. Sci., Part C: Polym. Lett.* **1990**, *28*, 213.
(28) Zhang, Y. X.; Da, A. H.; Butler, G. B.; Hogenesch, T. E. *J. Polym. Sci., Part A: Polym. Chem.* **1992**, *30*, 1383.
(29) Hwang, F. S.; Hogenesch, T. E. *Macromolecules* **1993**, *26*, 3156.
(30) Riess, J. G. *J. Fluorine Chem.* **2002**, *114*, 119.
(31) Riess, J. G. *Tetrahedron* **2002**, *58*, 4113.
(32) Okay, O.; Oppermann, W. *Macromolecules* **2007**, *40*, 3378.
(33) Amis, E. J.; Hu, N.; Seery, T. A. P.; Hogen-Esch, T. E.; Yassini, M.; Hwang, F. *Hydrophilic Polymers: Performance with Environmental Acceptance*; American Chemical Society: Washington, DC, 1996; Vol. 248.
(34) Mark, J. E.; Erman, B. *Rubberlike Elasticity: A Molecular Primer*; John Wiley & Sons, Inc.: New York, 1988.
(35) Gundogan, N.; Okay, O.; Oppermann, W. *Macromol. Chem. Phys.* **2004**, *205*, 814.
(36) Picout, D. R.; Ross-Murphy, S. B. In *Polymer Gels Networks*, Osada, Y., Khokhlov, A. R., Eds.; Marcel Dekker, Inc.: New York, 2002; p 34.
(37) Zhang, D. K.; Duan, J. J.; Wang, D. G.; Ge, S. R. *J. Bionic Eng.* **2010**, *7*, 235.
(38) Tsitsilianis, C.; Aubry, T.; Iliopoulos, I.; Norvez, S. *Macromolecules* **2010**, *43*, 7779.
(39) Xu, J. Y.; Liu, Z. S.; Erhan, S. Z. *J. Am. Oil Chem. Soc.* **2008**, *85*, 285.
(40) Williams, G.; Watts, D. C. *Trans. Faraday Soc.* **1970**, *66*, 80.
(41) Gurtovenko, A. A.; Gotlib, Y. Y. *J. Chem. Phys.* **2001**, *115*, 6785.
(42) Baeurle, S. A.; Hotta, A.; Gusev, A. A. *Polymer* **2005**, *46*, 4344.
(43) Winter, H. H. *Polym. Eng. Sci.* **1987**, *27*, 1698.